

PSFC/JA-03-22

**Toroidal Rotation and Momentum Transport in Alcator C-
Mod Plasmas with No Momentum Input**

Rice, J.E.; Lee†, W.D.; Marmor, E.S.; Basse, N.P.; Bonoli, P.T.;
Greenwald, M.J.; Hubbard, A.E.; Hughes, J.W.; Hutchinson, I.H.;
Ince-Cushman, A.; Irby, J.H.; Lin, Y.; Mossessian, D.; Snipes,
J.A.; Wolfe, S.M.; Wukitch, S.J.; and Zhurovich, K.

October 21, 2003

Plasma Science and Fusion Center
Massachusetts Institute of Technology
Cambridge, MA 02139 USA

†present address: Archimedes Technology Group, San Diego, CA

This work was supported by the U.S. Department of Energy,
Cooperative Grant No. DE-FC02-99ER54512. Reproduction,
translation, publication, use and disposal, in whole or in part, by or
for the United States government is permitted.

Submitted for publication to *Physics of Plasmas*.

Toroidal Rotation and Momentum Transport in Alcator C-Mod Plasmas with No Momentum Input

J. E. Rice, W. D. Lee[†], E. S. Marmor, N. P. Basse, P. T. Bonoli, M. J. Greenwald,
A. E. Hubbard, I. H. Hutchinson, A. Ince-Cushman, J. W. Hughes, J. H. Irby,
Y. Lin, D. Mossessian, J. A. Snipes, S. M. Wolfe, S. J. Wukitch and K. Zhurovich
Plasma Science and Fusion Center, MIT, Cambridge, MA 02139-4307

[†]present address: *Archimedes Technology Group, San Diego, CA*

Abstract

The time evolution of toroidal rotation velocity profiles has been measured in Alcator C-Mod [I. H. Hutchinson *et al.*, Phys. Plasmas **1**, 1511 (1994)] plasmas using a tangentially viewing x-ray spectrometer array. The strong co-current toroidal rotation in enhanced D_α (EDA) high confinement mode (H-mode) plasmas is observed to propagate in from the edge on a time scale similar to the energy confinement time. The ensuing steady state rotation velocity profiles in both Ohmic and ion cyclotron range of frequencies (ICRF) heated EDA H-modes, which are generated in the absence of any external momentum input, are found to be relatively flat. These profiles may be simulated by a simple diffusion model with the boundary condition of an edge rotation, which appears during the H-mode period. The observed profiles are well matched by the simulations using a momentum diffusivity of $\sim 0.1 \text{ m}^2/\text{s}$, which is much larger than the calculated neo-classical value, and the momentum transport may be regarded as anomalous. The Alcator C-Mod rotation observations have been compared in detail with the calculations of neo-classical and sub-neo-classical theory, to the predictions from modeling of ICRF wave induced energetic ion orbit shifts, and to estimates from turbulence driven mechanisms. The magnitude and scalings of the observed rotation results are in accord with neo-classical and sub-neo-classical calculations, but the measured momentum diffusivity is higher than the predictions by a large fraction. The prediction of rotation rever-

sal with a high magnetic field side resonance location for ICRF wave induced ion orbit shifts has not been observed in the experiments. While the turbulence driven rotation calculations are mostly qualitative, they represent some of the observed features.

I. Introduction

Rotation and velocity shear play important roles in the transition to high confinement mode (H-mode) [1-5], in suppression of resistive wall modes [6] and in the formation of internal transport barriers (ITBs) [7] in tokamak discharges. Even so, there has been considerably less effort addressing momentum transport compared to energy and particle transport. In a majority of tokamak plasmas, the observed toroidal rotation is generated externally by neutral beam injection [8-15]. Momentum confinement is generally found to be anomalous, with a diffusivity, χ_ϕ , similar to the ion thermal conductivity, χ_i [8-15], but much larger than the neo-classical diffusivity (viscosity). Despite the fact that there is no momentum input in Alcator C-Mod plasmas, ICRF [16,17] and Ohmic [16,18,19] H-mode discharges are found to have substantial spontaneous co-current toroidal impurity rotation. Similar observations have been made on other devices such as JET [20,21], COMPASS [22] and Tore Supra [23-25]. The Alcator C-Mod rotation results are summarized in the following. Lower single null Ohmic L-mode discharges are found to have a slight (~ 10 km/s) counter-current rotation [26], and the magnitude and direction are consistent with neo-classical theory [27]. ICRF and Ohmic H-mode plasmas exhibit co-current rotation up to 100 km/s, without direct momentum input. Following the L- to H-mode transition, the core rotation rises on a time scale of order of τ_E , the energy confinement time, with a magnitude proportional to the increase in the plasma stored energy normalized to the plasma current [17]. (A similar scaling has been found in Tore Supra [25].) The rotation reverses direction when the current direction is reversed [28]. The magnitude of the rotation is consistent with a core radial electric field, E_r , of +10s of kV/m. For H-mode discharges which evolve internal transport barriers (ITBs), the core rotation velocity and E_r change sign [28-30].

Several attempts to explain the observed rotation in C-Mod have been made, based on sub-neo-classical [31] effects, ICRF wave driven fast particle orbit shift mechanisms [32-35] and turbulence [36,37]. Quantitative comparisons of the pre-

dictions of each of these theories to the C-Mod observations will be made in Section IV after a presentation of the measurements in Section III. In section II the experimental setup is described and conclusions are drawn in Section V.

II. Experiment and Spectrometer Description

The observations presented here were obtained from the Alcator C-Mod tokamak, a compact (major radius $R_0 = 0.67$ m, typical minor radius $a = 0.21$ m), high magnetic field ($B_T \leq 8$ T) device with strong shaping capabilities and all metal plasma facing components. Auxilliary heating is available with 3 MW of ICRF heating power at 80 MHz, which is coupled to the plasma by 2 two-strap antennas. For the discharges described here, the hydrogen minority heating was with $0-\pi$ phasing, and there was no momentum input. An additional 3 MW of ICRF power are available from a variable frequency, variable phase four-strap antenna; for the cases described here, this antenna was operated at both 70 and 78 MHz with $0-\pi-0-\pi$ phasing, again with no momentum input. Previous off-axis toroidal rotation measurements from the Doppler shifts of argon x-ray lines on Alcator C-Mod were from x-ray spectrometers with only a slight toroidal view [16], so only large rotation velocities could be seen, and then only with poor time resolution. The x-ray crystal spectrometer system has now been modified with three fully tangential views, vertically displaced to provide three points on the rotation profile. The three spectrometers have views which are tangent to $R=0.685$ m, with chords on the mid-plane and vertically displaced by 0.09 and 0.18 m, respectively. With the mapping to the outboard horizontal mid-plane, the profile coverage is at $r/a = 0.0, 0.3$ and 0.6 . The central chord spectrometer observes the Ar^{17+} Ly_α doublet while the off-axis spectrometers monitor the Ar^{16+} forbidden line, z [16]. These three rotation measurements are augmented by the velocity of magnetic perturbations associated with sawtooth oscillations recorded with an array of fast pickup coils [18]. This provides rotation information at the $q=1$ surface, which is typically near $r/a \sim 0.2$. Electron density profiles were determined by Thomson scattering and

from the visible continuum using a high spatial resolution imaging charge coupled device system. Electron temperature profiles were determined from Thomson scattering and from electron cyclotron emission. Magnetic flux surface reconstructions were provided from the EFIT [38] code.

III. Observed Rotation Profile Evolution in EDA H-mode Plasmas

Plasma parameter time histories for a typical EDA H-mode [39] plasma are shown in Fig.1. This 5.4 T, 0.8 MA discharge entered H-mode at 0.657 s following application of 2 MW of 80 MHz ICRF power at 0.6 s. The usual signatures of H-mode were seen in the rise of the stored energy and electron density in conjunction with significant co-current toroidal rotation. The rotation velocity profile evolution for this discharge is shown in the top frame of Fig.2. The rotation increase was first seen at $r/a = 0.6$ (purple diamonds) immediately following the H-mode transition. The rotation subsequently propagated into the interior and settled into a flat profile after 150 ms or so [40,41]. This profile time development is suggestive of the evolution of an edge source of momentum governed by a diffusive process.

The evolution of the toroidal rotation velocity profile in EDA H-mode plasmas has been simulated using a simple source-free momentum transport model [40] (in cylindrical coordinates)

$$\frac{\partial}{\partial t}P - \frac{1}{r} \frac{\partial}{\partial r}(rD_\phi \frac{\partial}{\partial r}P) = 0$$

with $P = n_i m_i V_\phi$, and where the momentum diffusivity, D_ϕ , is a free parameter to be determined. Subject to the boundary conditions of an edge rotation, V_0 , which is present only during H-mode

$$V_\phi(a, t) = V_0 \quad , \quad t_{L \rightarrow H} \leq t \leq t_{H \rightarrow L}.$$

(a is the minor radius) and with the assumptions (observed in the electrons) of a flat ion density profile and constant (spatially and temporally) D_ϕ , the toroidal rotation velocity, $V_\phi(r,t)$, profile evolution may be determined from a solution to

$$\frac{\partial}{\partial t} V_\phi - D_\phi \left[\frac{\partial^2}{\partial r^2} V_\phi + \frac{1}{r} \frac{\partial}{\partial r} V_\phi \right] = 0$$

via an expansion in Bessel functions. An example of the results of this modeling is shown in the bottom of Fig.2, where D_ϕ was determined to be $0.1 \text{ m}^2/\text{s}$, with $\tau_\phi \sim 75$ ms. The simulation well reproduces the propagation in from the edge, the resultant steady flat profiles and the overall time scale for the evolution. This momentum diffusivity is much larger than the classical estimate [42] $\chi_\phi \sim \rho_i^2 / \tau_{ii} \sim 0.003 \text{ m}^2/\text{s}$ (the neo-classical value is even smaller) and the observed momentum transport may be considered as highly anomalous, a result seen in many tokamak experiments.

IV. Comparisons with Theory

The C-Mod rotation observations in Ohmic L-mode plasmas [26] have previously been compared to the predictions of neo-classical theory [27]. The calculated magnitude, direction (counter-current) and independence on the mass of the impurity ions were found to be in agreement with the experiment for discharges with a lower single null. Upper single null and limited plasmas have substantial counter-current rotation, $\sim -40 \text{ km/s}$ [41] and for these configurations, the magnitude is not in good agreement with neo-classical theory. In the case of H-mode plasmas, the observed scaling of the rotation, proportional to the inverse of the plasma current [17,18,25] is in qualitative agreement with the scalings of neo-classical theory [27]. The magnitude of the rotation is proportional to the radial electric field, which is not calculated in a self-consistent manner (left as a free parameter), and the rotation measurements can be used to infer E_r , which is a common practice in many tokamak experiments. For C-Mod, it is typically in the range of $+ 10\text{-}30 \text{ kV/m}$ in the core of H-mode discharges and -10 kV/m in ITB plasmas [28,30]. In spite of these areas of agreement (which may be fortuitous), the large discrepancy in the calculated and measured momentum diffusivity indicates that another process is dominating momentum transport, to levels well above neo-classical. Furthermore, the ordering

assumed in the original neo-classical derivation is violated, since the temperature gradient scale length is less than the ion gyro-radius in the edge of C-Mod H-mode discharges. This ordering has been properly treated in the sub-neo-classical theory [43,44], which also provides E_r from an ambipolarity constraint. The toroidal rotation velocity profile may also be determined and is proportional to the temperature gradient. The sub-neo-classical theory [31] correctly predicts the magnitude, direction and scaling for the observed rotation in many Ohmic H-mode discharges. However there are some plasmas where the agreement is not so good; one such case is shown in Fig.3. This particular Ohmic discharge had an edge localized mode free (ELM-free) H-mode period between 1.1 and 1.25 s, which demonstrated strong co-current rotation, ~ 40 km/s, and an EDA H-mode period between 1.3 and 1.5 s, which had substantially lower rotation, ~ 10 km/s. The edge electron temperature profiles for these two time periods were nearly identical, as shown in Fig.4. Eq.17 of [31] would predict the core toroidal rotation velocities to be the same, which is not observed. Apparently there is another factor during these two different H-mode periods which is governing the rotation. Similar to the standard neo-classical theory, the momentum diffusivity in the sub-neo-classical theory is also much below the observed value.

Another approach toward explanation of the co-current rotation in ICRF heated H-mode discharges is through the toroidal torque provided by the radial electric field due to orbit shifts of high energy ions generated by ICRF waves [32-35]. A particular prediction of some of these theories [33,35] is that the rotation should switch direction to counter-current with the ICRF resonance located on the high magnetic field side (HFS). The resonance location has been moved by varying the toroidal magnetic field [28,29]. Shown in Fig.5 is a comparison of two H-mode discharges produced by 1.5 MW of ICRF power at 70 MHz. For the plasma shown in green, the resonance was on the magnetic axis for 4.5 T and there were the usual characteristics of stored energy increase and co-current rotation. The discharge shown in red (4.0 T) exhibited very similar co-current rotation even though the resonance location was $(R-R_0)/a \sim -0.4$ on the HFS, in contrast to the predictions. Oper-

ation with the ICRF resonance outside of $|r/a| = 0.5$ led to the discovery of ITB plasmas in C-Mod [28,29], however. The similarities in the rotation observations (magnitude and scalings) in Ohmic and ICRF heated H-mode plasmas suggest that it is not an ICRF wave or fast particle effect.

An alternative approach to explain the spontaneous generation of rotation is based on turbulence. Fluctuation induced toroidal stress [36] can give rise to toroidal rotation and the direction of the rotation depends upon the mode frequency spectrum, which may explain the reversal of the observed rotation in going from L- to H-mode. If the Doppler shifted mode frequency is of order of the ion diamagnetic drift frequency, ω^*_i , the calculated velocity profile is predicted to have a shape proportional to the temperature profile, raised to the 5/2 power (Eq.15 of [36]). This is not what is observed in the profile for the EDA H-mode discharge shown in Figs.1 and 2, as can be seen in the top frame of Fig.6. The observed flat rotation profile is compared to the measured electron temperature shape raised to the 5/2 power, and the agreement is not good. One characteristic of EDA H-mode plasmas is the appearance of the quasi-coherent (QC) mode [45-47] very close to the plasma edge, with a frequency near 100 kHz. $\omega^*_i/2\pi$ for the EDA H-mode discharge of Figs.1 and 2 as a function of radius is shown in Fig.7. The QC mode frequency is very close to $\omega^*_i/2\pi$ at the edge of this EDA discharge, so the calculated velocity profile might be expected to match the observed one. However, not much is known about the turbulence spectrum in the core of EDA H-mode plasmas. In the case of ELM-free H-mode discharges, the rotation profiles are peaked at the magnetic axis [16,40,41] and the observed rotation profiles are well represented by $(T_e)^{5/2}$. One such comparison [40,41] is shown in the bottom frame of Fig.6. $\omega^*_i/2\pi$ for this ELM-free discharge is also shown in Fig.7 and is very similar to the EDA case. In ELM-free H-mode plasmas there is no edge QC mode with a frequency near 100 kHz, so the above condition is not valid at the plasma edge, but, ironically, the observed rotation profile in this case is in good agreement with the calculated $(T)^{5/2}$ scaling. Again, not much is known about the core turbulence in ELM-free H-mode discharges, so the comparisons of Fig.6 may not be justified.

A similar model [37] of electrostatic modes driven by the ion pressure gradient is in qualitative agreement with many of the features observed in the C-Mod experiment: direction of rotation in L- and H-mode, scaling with W_P/I_P in H-mode and the drop in the rotation observed in ITB plasmas. However, there are no quantitative predictions about the magnitude of the rotation or the size of the momentum diffusivity for further comparison with the experimental results.

Finally, in another approach to explain the enhanced momentum diffusivity, the effects of neutral viscosity have been found to dominate the ion viscosity [48], but no quantitative comparisons have been made with the C-Mod observations at this time.

VI. Discussion and Conclusions

Spontaneous co-current toroidal rotation has been observed in the interior of Alcator C-Mod H-mode discharges with no external momentum input. In EDA H-mode plasmas, the rotation propagates in from the plasma edge on a time scale similar to the energy confinement time, and evolves to a flat rotation profile. In ELM-free discharges, the rotation profiles are centrally peaked. Comparison of the EDA H-mode observations with a simple diffusion model indicates that the momentum diffusivity is of order $0.1 \text{ m}^2/\text{s}$, much larger than the neo-classical value, and the momentum transport may be regarded as anomalous. The similarity between observations in Ohmic and ICRF heated H-mode discharges suggests that the rotation is not due to ICRF effects. In fact the prediction of certain ICRF orbit shift models that the rotation direction should switch to counter-current with the wave resonance on the high magnetic field side has not been observed in the experiments. Certain features of the experimental rotation observations are in qualitative agreement with theoretical predictions based on turbulence effects.

V. Acknowledgements

The authors thank J. Terry for D_α measurements, S. Scott for useful discussions

and the Alcator C-Mod operations and ICRF groups for expert running of the tokamak. Work supported at MIT by DoE Contract No. DE-FC02-99ER54512.

References

- [1] K.C.Shaing and E.C.Crume, Phys. Rev. Lett. **63**, 2369 (1989).
- [2] H.Biglari, P.H.Diamond and P.W.Terry, Phys. Fluids **B2**, 1 (1990).
- [3] R.J.Groebner, K.H.Burrell and R.P.Seraydarian, Phys. Rev. Lett. **64**, 3015 (1990).
- [4] K.Ida, S.Hidekuma, Y.Miura *et al.*, Phys. Rev. Lett. **65**, 1364 (1990).
- [5] P.W.Terry, Rev. Mod. Phys. **72**, 109 (2000).
- [6] E.J.Strait, T.S.Taylor, A.D.Turnbull *et al.*, Phys. Rev. Lett. **74**, 2483 (1994).
- [7] K.Burrell, Phys. Plasmas **4**, 1499 (1997).
- [8] S.Suckewer, H.P.Eubank, R.J.Goldston *et al.*, Nucl. Fusion **21**, 1301 (1981).
- [9] K.H.Burrell, R.J.Groebner, H.St.John and R.P.Seraydarian, Nucl. Fusion **28**, 3 (1988).
- [10] S.D.Scott, P.H.Diamond, R.J.Fonck *et al.*, Phys. Rev. Lett **64**, 531 (1990).
- [11] A.Kallenbach, H.M.Mayer, G.Fussmann *et al.*, Plasma Phys. Contr. Fusion **33**, 595 (1991).
- [12] N.Asakura, R.J.Fonck, K.P.Jaehrig, *et al.*, Nucl. Fusion **33**, 1165 (1993).
- [13] K.Nagashima, Y.Koide and H.Shirai, Nucl. Fusion **34**, 449 (1994).
- [14] K.-D.Zastrow, W.G.F.Core, L.-G.Eriksson, *et al.*, Nucl. Fusion **38**, 257 (1998).
- [15] J.S.deGrassie, D.R.Baker, K.H.Burrell *et al.*, Nucl. Fusion **43**, 142 (2003).
- [16] J.E.Rice, M.Greenwald, I.H.Hutchinson *et al.*, Nucl. Fusion **38**, 75 (1998).
- [17] J.E.Rice, P.T.Bonoli, J.A.Goetz *et al.*, Nucl. Fusion **39**, 1175 (1999).
- [18] I.H.Hutchinson, J.E.Rice, R.S.Granetz and J.A.Snipes, Phys. Rev. Lett. **84**, 3330 (2000).
- [19] J.E.Rice, J.A.Goetz, R.S.Granetz *et al.*, Phys. Plasmas **7**, 1825 (2000).
- [20] L.-G.Eriksson, E.Righi and K.D.Zastrow, Plasma Phys. Contr. Fusion **39**, 27 (1997).
- [21] J.-M.Noterdaeme, E.Righi, V.Chan *et al.*, Nucl. Fusion **43**, 274 (2003).
- [22] I.H. Coffey, R. Barnsley, F.P. Keenan *et al.*, in Proceedings of the 11th Colloquium on UV and X-ray Spectroscopy of Astrophysical and Laboratory Plasmas,

Nagoya, Japan, 1995, p.431, Frontiers Science Series No.15 (Editors: K. Yamashita and T. Watanabe), Universal Academy Press, Tokyo, Japan, 1996

- [23] G.T.Hoang, P.Monier-Garbet, T.Aniel *et al.*, Nucl. Fusion **40**, 913 (1999).
- [24] L.-G.Eriksson, G.T.Hoang and V.Bergeaud, Nucl. Fusion **41**, 91 (2001).
- [25] S.Assas, C.Fenzi-Bonizec, L.-G.Eriksson and G.T.Hoang, 'Toroidal plasma rotation in ICRF heated Tore Supra discharges', 30th European Physical Society Conference on Plasma Physics and Controlled Fusion, St. Petersburg, Russia, 7-11 July 2003, ECA Vol. **27A** P-1.138
- [26] J.E.Rice, E.S.Marmar, F.Bombarda and L.Qu, Nucl. Fusion **37**, 421 (1997).
- [27] Y.B.Kim, P.H.Diamond and R.J.Groebner, Phys. Fluids **B3**, 2050 (1991).
- [28] J.E.Rice, R.L.Boivin, P.T.Bonoli *et al.*, Nucl. Fusion **41**, 277 (2001).
- [29] J.E.Rice, P.T.Bonoli, E.S.Marmar *et al.*, Nucl. Fusion **42**, 510 (2002).
- [30] J.E.Rice, P.T.Bonoli, C.L.Fiore *et al.*, Nucl. Fusion **43**, 781 (2003).
- [31] A.L.Rogister, J.E.Rice, A.Nicolai *et al.*, Nucl. Fusion **42**, 1144 (2002).
- [32] C.S.Chang, C.K.Phillips, R.White *et al.*, Phys. Plasmas **6**, 1969 (1999).
- [33] F.W.Perkins, R.B.White, P.T.Bonoli and V.S.Chan, Phys. Plasmas **8**, 2181 (2001).
- [34] V.S.Chan, S.C.Chiu and Y.A.Omelchenko, Phys. Plasmas **9**, 501 (2002).
- [35] L.-G.Eriksson and F.Porcelli, Nucl. Fusion **42**, 959 (2002).
- [36] K.C.Shaing, Phys. Rev. Lett. **86**, 640 (2001).
- [37] B.Coppi, Nucl. Fusion **42**, 1 (2002).
- [38] L.L.Lao, H.St.John, R.Stambaugh *et al.*, Nucl. Fusion **25**, 1611 (1985).
- [39] M.Greenwald, R.L.Boivin, F.Bombarda *et al.*, Nucl. Fusion **37**, 793 (1997).
- [40] W.D.Lee, J.E.Rice, E.S.Marmar *et al.*, 'Observations of Anomalous Momentum Transport in Tokamak Plasmas with No Momentum Input', to appear in Phys. Rev. Lett. (2003).
- [41] J.E.Rice, W.D.Lee, E.S.Marmar *et al.*, 'Observations of Anomalous Momentum Transport in Alcator C-Mod Plasmas with No Momentum Input', submitted to Nucl. Fusion (2003).
- [42] F.L.Hinton and S.K.Wong, Phys. Fluids **28**, 3088 (1985).

- [43] A.L.Rogister, Phys. Plasmas **6**, 200 (1999).
- [44] H.A.Claassen, H.Gerhauser, A.Rogister and C.Yarim, Phys. Plasmas **7**, 3699 (2000).
- [45] M.Greenwald, R.Boivin, P.Bonoli *et al.*, Phys. Plasmas **6**, 1943 (1999).
- [46] J.A.Snipes, B.LaBombard, M.Greenwald *et al.*, Plasma Phys. Contr. Fusion **43**, L23 (2001).
- [47] A.Mazurenko, M.Porkolab, D.Mosessian *et al.*, Phys. Rev. Lett. **89**, 225004 (2002).
- [48] R.D.Hazeltine, M.D.Calvin, P.M.Valanju and E.R.Solano, Nucl. Fusion **32**, 3 (1992).

Figure Captions

Fig. 1 Time histories for an EDA H-mode plasma generated with 2 MW of ICRF power. From top to bottom the plasma stored energy, central electron density, central electron temperature, D_α brightness and central toroidal rotation velocity. The waveform of the ICRF pulse is shown in green in the middle frame.

Fig. 2 The time evolution of the toroidal rotation velocity at four spatial locations for the discharge of Fig.1 are shown in the top frame. The argon x-ray Doppler shift measurements for $r/a = 0.0, 0.3$ and 0.6 are depicted by the red dots, green asterisks and purple diamonds, respectively. The rotation from sawtooth pre-cursors at the $q=1$ surface, $r/a \sim 0.2$, are shown by the black \times s. Representative error bars are depicted. In the bottom frame are simulations of the x-ray data with $D_\phi = 0.1 \text{ m}^2/\text{s}$.

Fig. 3 Time histories for an Ohmic discharge which had an ELM-free H-mode period from 1.10 to 1.24 s, and an EDA H-mode period from 1.30 to 1.49 s. From top to bottom are the plasma stored energy, central electron density, toroidal magnetic field, plasma current, D_α brightness and central toroidal rotation velocity.

Fig. 4 Edge electron temperature profiles for the discharge of Fig.3. Red asterisks are from the ELM-free H-mode at 1.2 s and green dots are from the EDA H-mode at 1.4 s.

Fig. 5 A comparison of two discharges with 1.5 MW of ICRF power at 70 MHz, with on-axis absorption (4.5 T, green) and with the resonance on the high field side at $(R-R_0)/a \sim -0.4$ (4.0 T, red). From top to bottom are the plasma stored energies, ICRF waveforms and central toroidal rotation velocities.

Fig. 6 A comparison of toroidal rotation velocity profiles in the EDA H-mode plasma of Figs.1 and 2 at 0.9 s (top) and an ELM-free H-mode discharge (bottom).

The solid curves are proportional to $(T_e)^{5/2}$.

Fig. 7 The ion diamagnetic drift frequency, ω^*_i , (divided by 2π) for the EDA plasma of Fig.6 (top) is shown in green, and for the ELM-free discharge of Fig.6 (bottom) is shown in red.

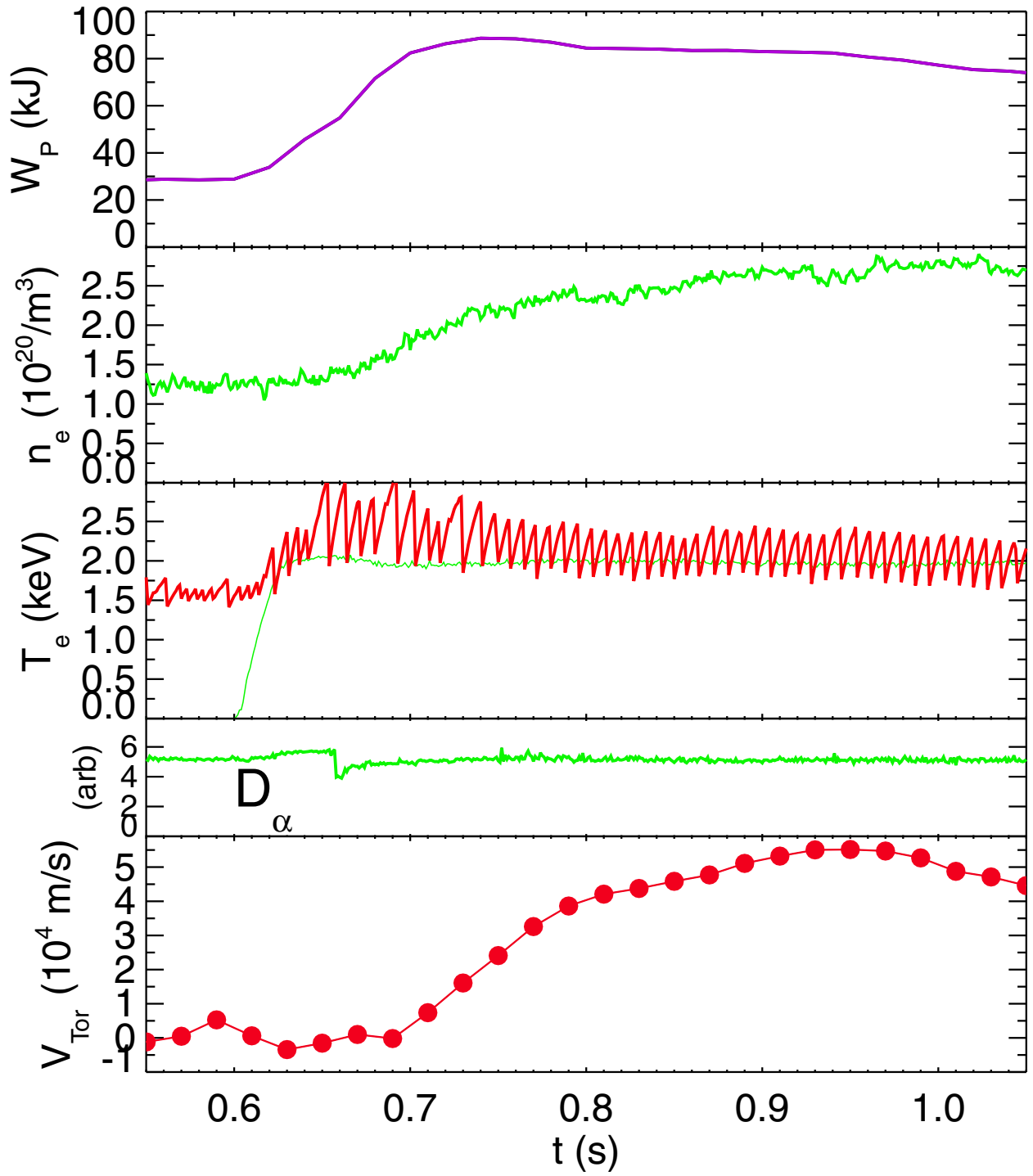


Figure 1

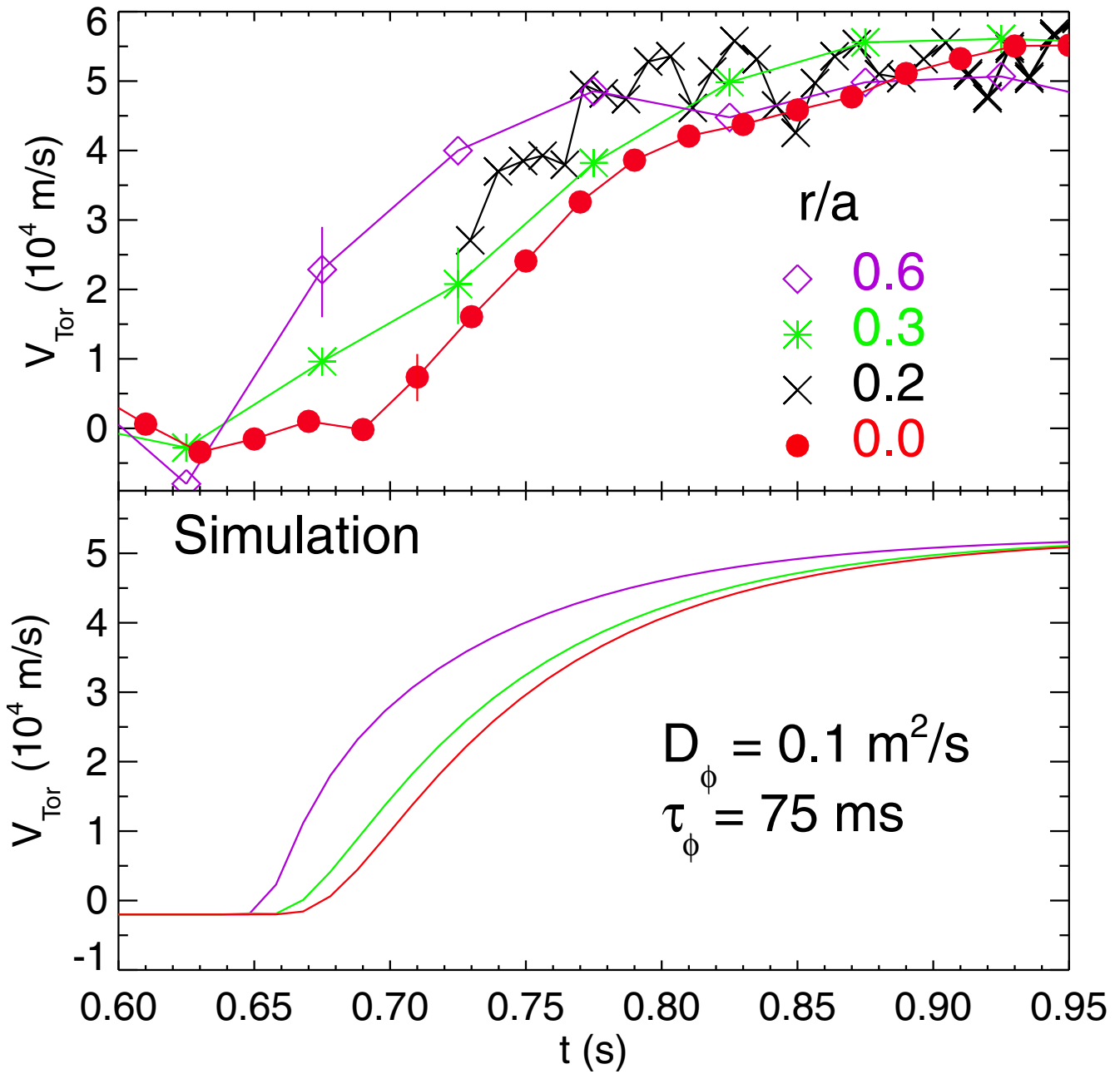


Figure 2

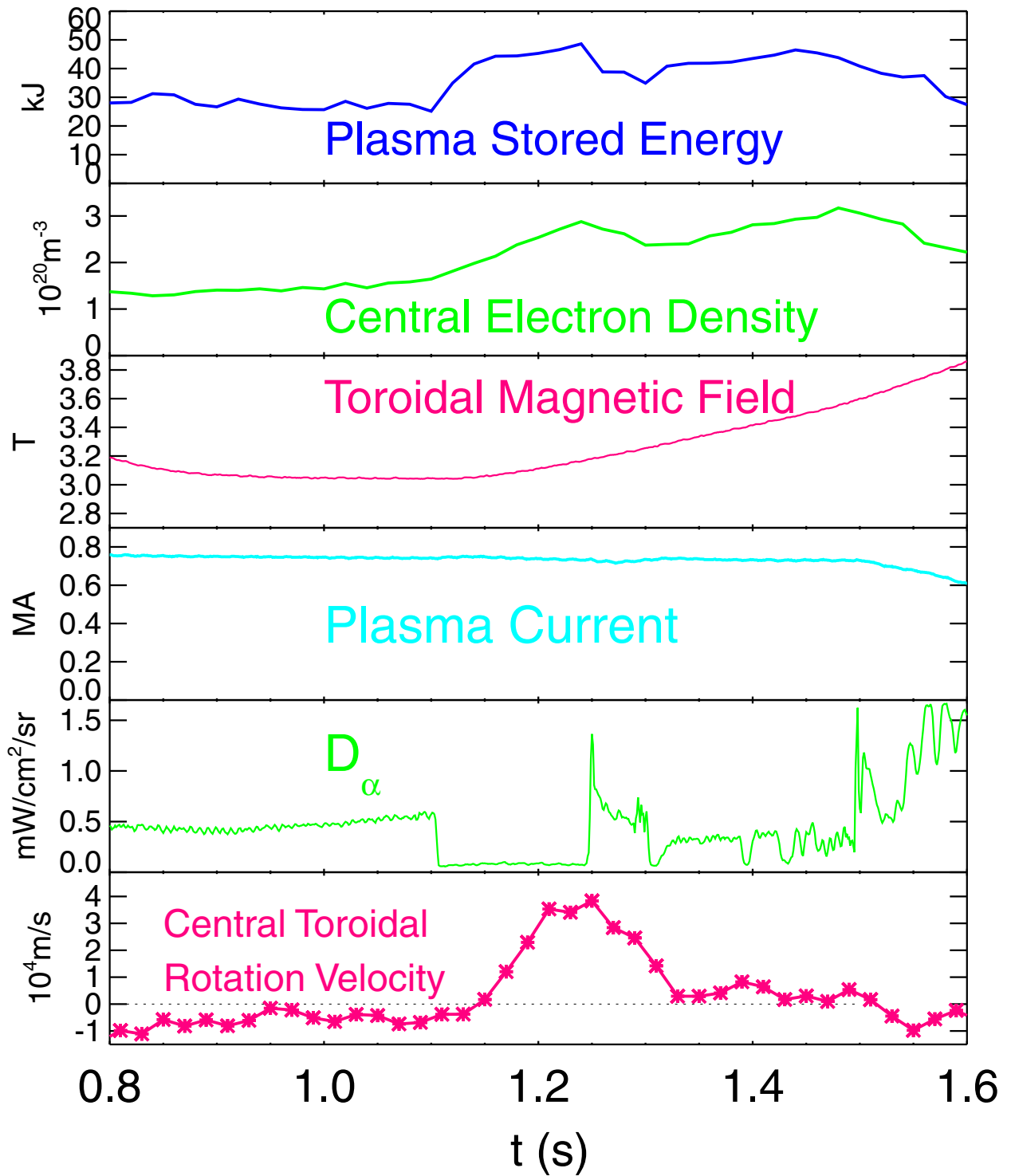


Figure 3

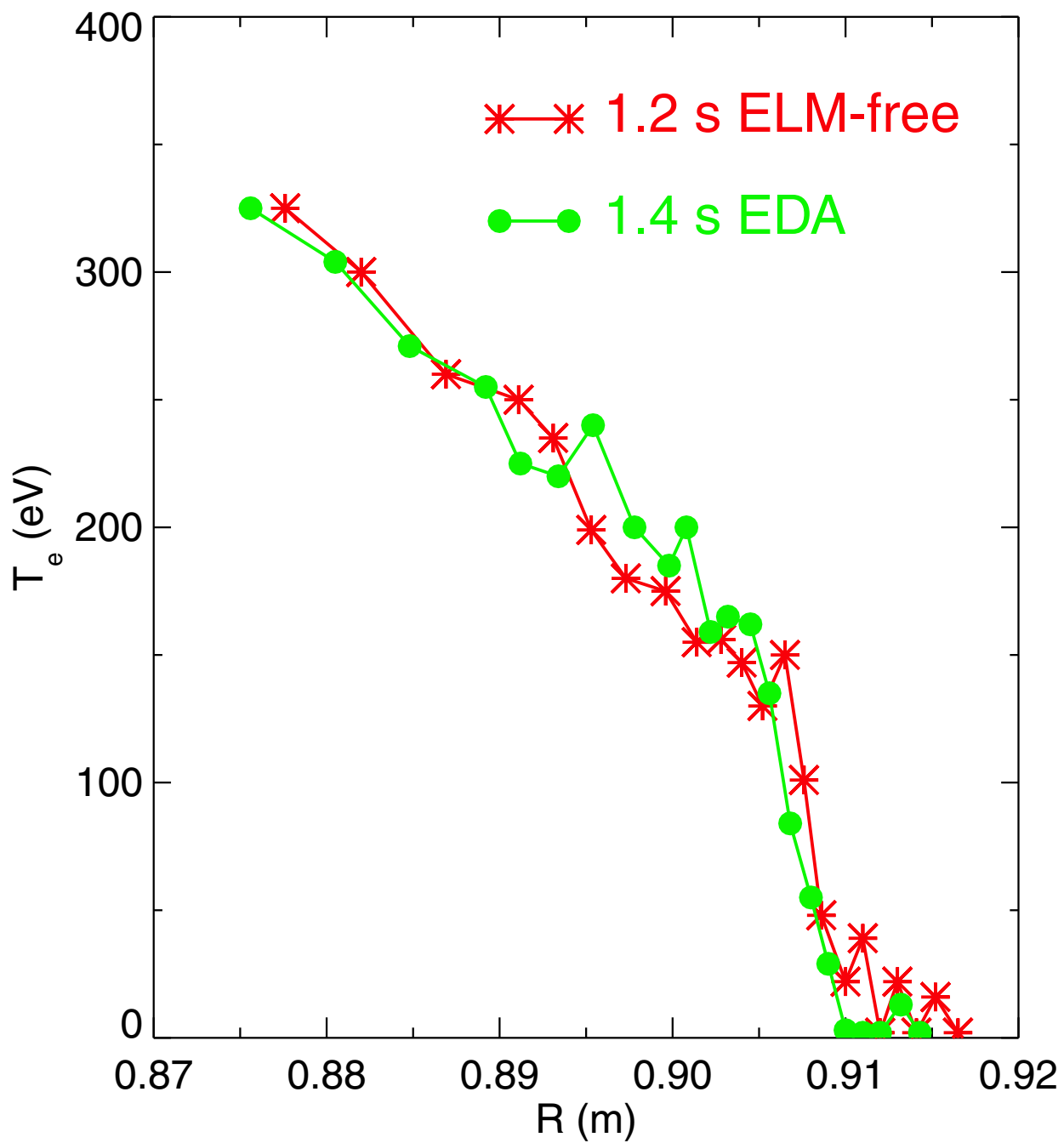


Figure 4

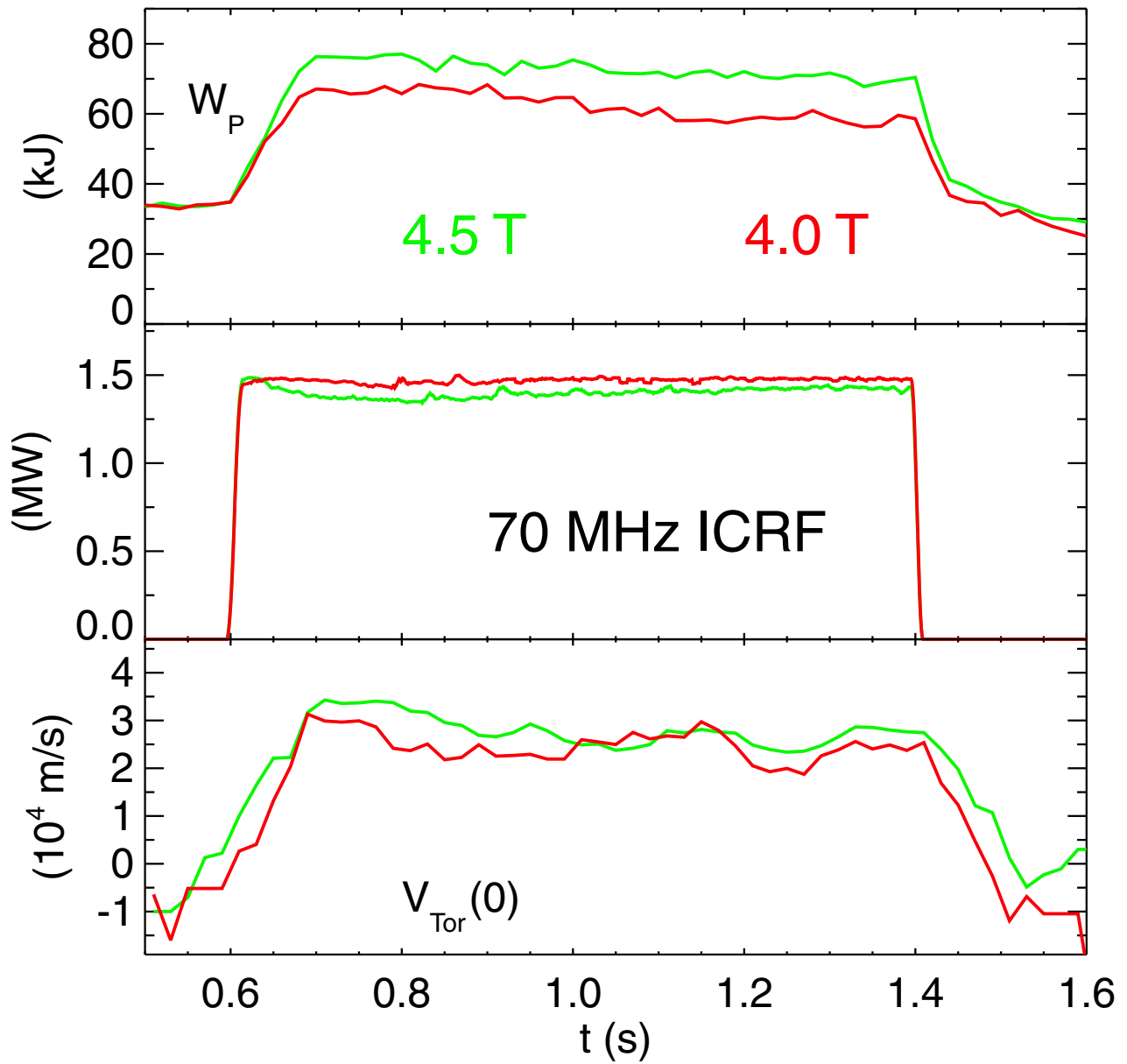


Figure 5

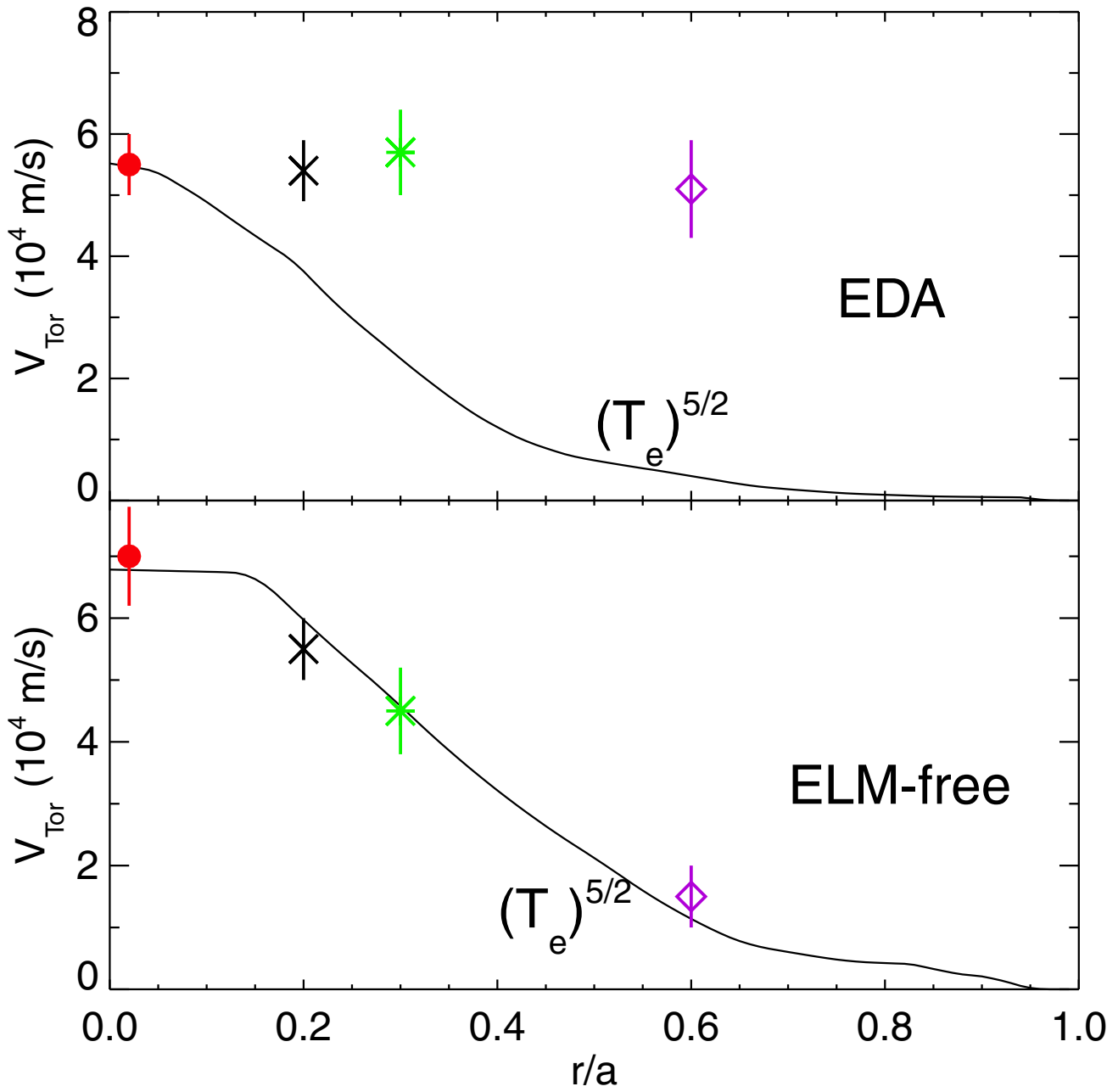


Figure 6

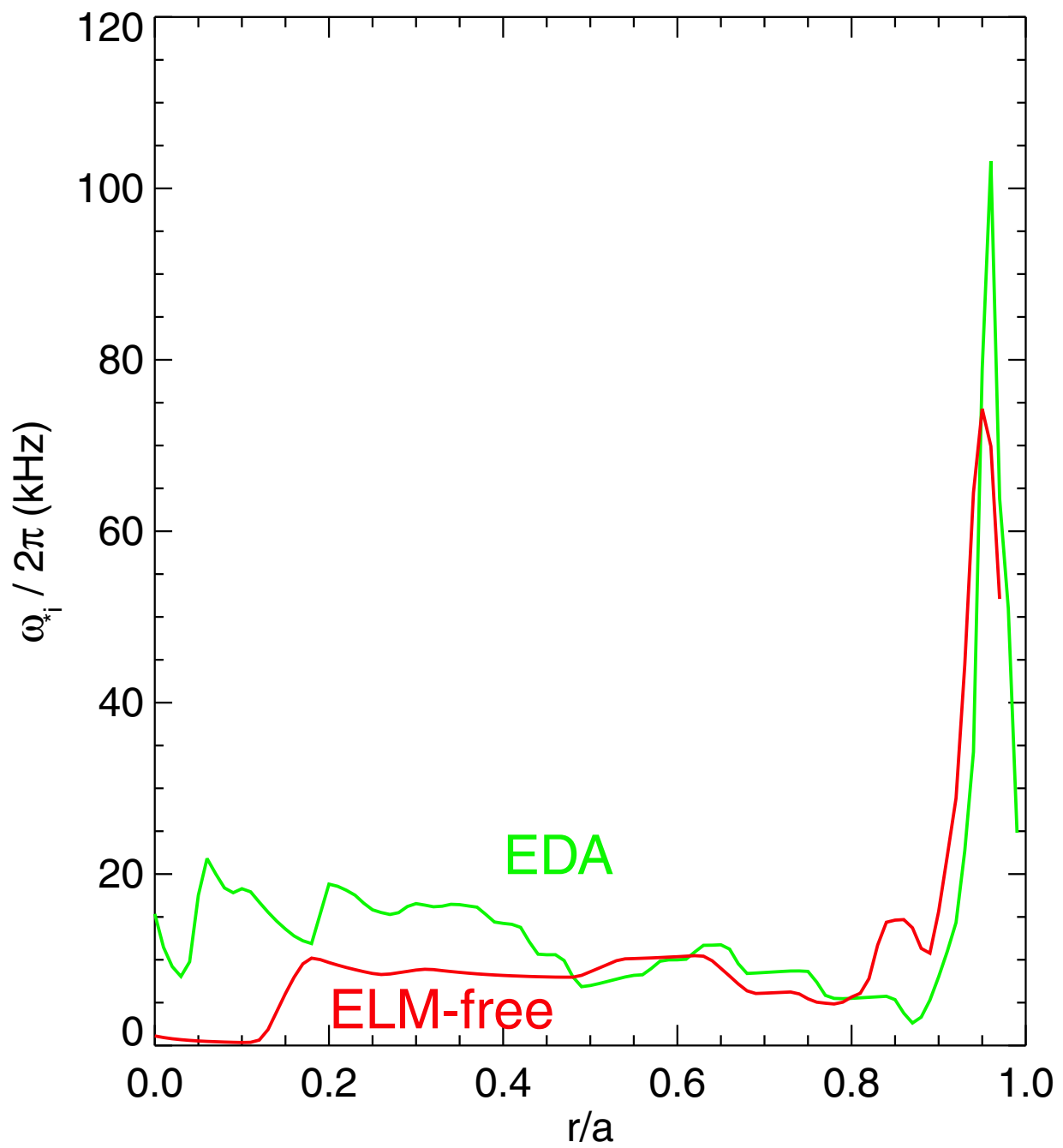


Figure 7